



저작자표시-비영리-변경금지 2.0 대한민국

이용자는 아래의 조건을 따르는 경우에 한하여 자유롭게

- 이 저작물을 복제, 배포, 전송, 전시, 공연 및 방송할 수 있습니다.

다음과 같은 조건을 따라야 합니다:



저작자표시. 귀하는 원저작자를 표시하여야 합니다.



비영리. 귀하는 이 저작물을 영리 목적으로 이용할 수 없습니다.



변경금지. 귀하는 이 저작물을 개작, 변형 또는 가공할 수 없습니다.

- 귀하는, 이 저작물의 재이용이나 배포의 경우, 이 저작물에 적용된 이용허락조건을 명확하게 나타내어야 합니다.
- 저작권자로부터 별도의 허가를 받으면 이러한 조건들은 적용되지 않습니다.

저작권법에 따른 이용자의 권리는 위의 내용에 의하여 영향을 받지 않습니다.

이것은 [이용허락규약\(Legal Code\)](#)을 이해하기 쉽게 요약한 것입니다.

[Disclaimer](#)

공학석사학위논문

케이싱 형상이 쉬라우드형 터빈의  
공력성능에 미치는 효과

Effects of Casing Geometry on Shrouded Turbine  
Aerodynamic Performance

2023년 2월

서울대학교 대학원

기계공학부

이 창 열

# 케이싱 형상이 쉬라우드형 터빈의 공력성능에 미치는 효과

Effects of Casing Geometry on Shrouded Turbine  
Aerodynamic Performance

지도교수 송 성 진

이 논문을 공학석사 학위논문으로 제출함

2022년 10월

서울대학교 대학원

기계공학부

이 창 열

이 창 열의 공학석사 학위논문을 인준함

2022년 12월

위원장 :           최 해 천           (인)

부위원장 :           송 성 진           (인)

위 원 :           박 형 민           (인)

## Abstract

# Effects of Casing Geometry on Shrouded Turbine Aerodynamic Performance

Changyoul Lee

Department of Mechanical Engineering

The Graduate School

Seoul National University

This study aims to examine how the casing geometry affects turbine performance. In addition to the baseline geometry, two additional geometries are examined. In the first case with a slanted edge in the outlet cavity, the stage efficiency increases by 1.6%, and the mass fraction of the cavity flow decrease by 2.7% relative to the baseline geometry. In the second case with a rectangular corner in the inlet cavity, the efficiency increases by 1.0%, and the mass fraction of cavity flow decreases by 2.7%. Both cases achieve improvements in efficiency by reducing leakage mass flow rate. In both cases, efficiency was improved by reducing the cavity leakage mass flow rate, and in this paper, the cause of the decrease in the cavity leakage flow rate and the cause of the efficiency improvement is explained through detailed flow structure analysis.

**Keywords:** Shrouded turbine, Casing geometry, Aerodynamic loss, Cavity flow rate

**Student Number:** 2021-23581

# Table of Contents

<b>Abstract .....</b>	<b>iii</b>
<b>Chapter 1. Introduction .....</b>	<b>1</b>
1.1 Background .....	1
1.2 Previous research.....	3
1.3 Research objectives .....	7
<b>Chapter 2. Research method.....</b>	<b>8</b>
2.1 Numerical model .....	8
2.2 Numerical method .....	9
2.3 Casing design .....	10
<b>Chapter 3. Results.....</b>	<b>12</b>
3.1 Cavity flow mass fraction and efficiency .....	12
3.2 Total pressure loss coefficient .....	13
3.3 Pressure distribution .....	18
3.4 Torque.....	21
<b>Chapter 4. Conclusion .....</b>	<b>23</b>
<b>Reference .....</b>	<b>24</b>
<b>초록 .....</b>	<b>27</b>

# List of Figures

<b>Figure 1 Schematic of shrouded turbine.....</b>	<b>1</b>
<b>Figure 2 Schematic of the shroud geometry [2] .....</b>	<b>2</b>
<b>Figure 3 Casing geometry variation reducing cavity volume: (a) reducing outlet cavity gap (b) shroud cavity depth variation [3] .....</b>	<b>3</b>
<b>Figure 4 Casing geometrical concepts: (a) axial deflector (b) profiled end-wall [4] .....</b>	<b>4</b>
<b>Figure 5 Schematic of turbine cross section with inserts [5]....</b>	<b>5</b>
<b>Figure 6 Schematic of turbine cross section with stator casing extension [6] .....</b>	<b>6</b>
<b>Figure 7 Schematic of shroud geometry .....</b>	<b>9</b>
<b>Figure 8 Numerical computational domain: single passage</b>	<b>1 0</b>
<b>Figure 9 Schematic of the baseline case .....</b>	<b>1 1</b>
<b>Figure 10 Schematic of modified casing design : (a) slanted outlet cavity (b) stepped inlet cavity .....</b>	<b>1 1</b>
<b>Figure 11 Total pressure loss coefficient of baseline .....</b>	<b>1 5</b>
<b>Figure 12 Total pressure loss coefficient of slanted outlet cavity .....</b>	<b>1 6</b>

<b>Figure 13 Total pressure loss coefficient of stepped inlet cavity</b> .....	1 7
<b>Figure 14 Cavity region pressure distribution of baseline ...</b>	1 9
<b>Figure 15 Cavity region pressure distribution of slanted outlet cavity .....</b>	1 9
<b>Figure 16 Cavity region pressure distribution of stepped inlet cavity .....</b>	2 0
<b>Figure 17 Flow schematics in the relative frame.....</b>	2 1

## List of Tables

<b>Table 1 Turbine blade information.....</b>	8
<b>Table 2 Numerically calculated efficiency and cavity flow mass fraction.....</b>	1 3
<b>Table 3 Total pressure loss coefficient of each case(3.0 chord downstream from the rotor trailing edge).....</b>	1 4
<b>Table 4 Relative flow angle &amp; torque calculated by flow angle .....</b>	2 2



# Chapter 1. Introduction

## 1.1 Background

In a turbine, the rotor should rotate relative to the stationary casing. Since a gap is necessary between them. When the main flow goes through the blade passage, flow leaks into this gap. The loss associated with this leakage flow charges up to one third of the total turbine loss.

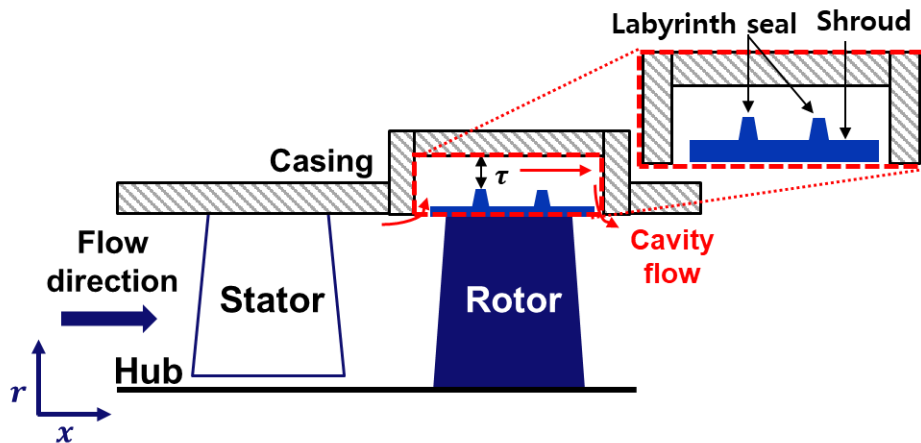
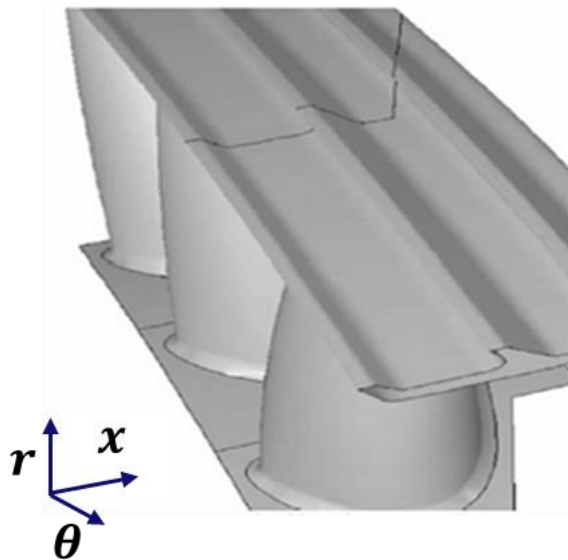


Figure 1 Schematic of shrouded turbine

A shrouded turbine blade is actively used in a modern gas turbine to decrease the tip leakage flow. Figure 1 shows a schematic of a generic shrouded turbine. In a shrouded turbine, there is a cover called a shroud. And it prevents main flow from leaking in the blade passage. 3D geometry of the generic shrouded turbine is shown in Figure 2 [2]. The shrouded turbine also has a gap between the labyrinth seals and casing. Hence, the main flow leaks through this gap. Leakage of the main flow is a direct loss of turbine work.

When this leakage flow re-enters the main flow path, a mixing loss is generated by the interaction between this leakage flow and main flow. For this reason, the leakage flow rate should be reduced to lessen the loss by mixing. Decreasing the seal gap and using multiple seals is a way to decrease the leakage mass flow rate. However, those methods have structural limitations. Hence it is important to figure out an optimized geometrical parameter to decrease the leakage flow that goes through the cavity.



**Figure 2 Schematic of the shroud geometry [2]**

## 1.2. Previous research

Several studies have been done to figure out the geometrical parameter to reduce the cavity mass flow rate and improve shrouded turbine performance.

Rosic et al. [3] aimed to figure out the effect of casing and shroud geometry on the turbine performance of the generic shroud turbine. They investigated the performance of various geometrical differential cases and found that minimizing the cavity volume by reducing the inlet and outlet cavity gap is effective to increase turbine efficiency. Also, Rosic et al. [4] found some geometrical variation concepts that increase turbine performance. Figure 4 shows his concepts, one of the axial deflector concepts improved turbine efficiency by 0.4% and one of the profiled end-wall concepts also increased turbine efficiency by 0.4%.

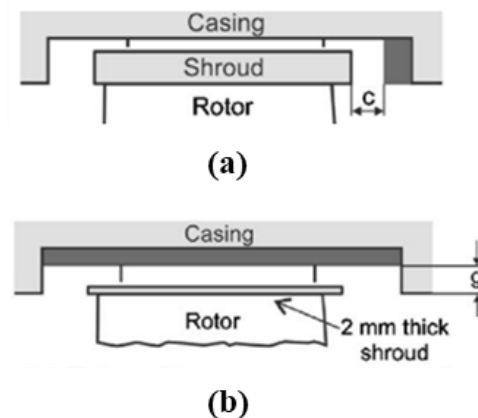


**Figure 3 Casing geometry variation reducing cavity volume: (a) reducing outlet cavity gap (b) shroud cavity depth variation [3]**

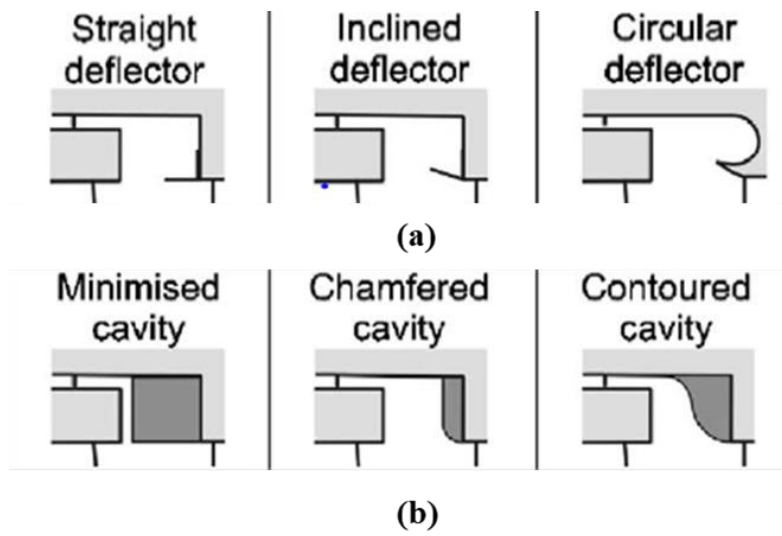


**Figure 4 Casing geometrical concepts: (a) axial deflector (b) profiled end-wall [4]**

Schlienger et al. [5] examined the effect of variation on cavity region by adding inserts in the shroud hub and rotor tip cavity outlet. Figure 5 shows the schematic of turbine geometry. Experimental results showed the total effect of inserts reduced the turbine efficiency. The hub inserts reduced mixing loss and secondary flow of the downstream flow field, however, tip inserts enhanced both of them. These two effects counterbalanced each of them.

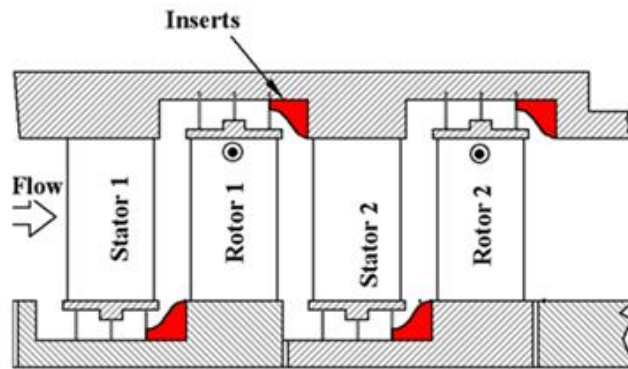


**Figure 5 Schematic of turbine cross section with inserts [5]**

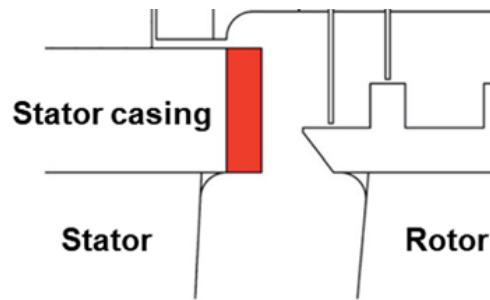


**Figure 6 Schematic of turbine cross section with stator casing extension [6]**

Barmपालias et al.[6] examined the effect of decreasing volume of the cavity inlet by extending stator casing length. In this paper, inlet cavity volume reduction induced transformation of the inlet cavity flow structure. And also the turbine efficiency is changed. In the 14% volume reduction case, the efficiency increased by 0.3%. However, the turbine efficiency decreased in the 28% volume reduction case.

Palmer et al. [7] figured out a quantitative mechanism of viscous entropy generation in cavity flow vortices and suggested a connection between the inlet cavity size and the vorticity.

### **1.3 Research objectives**

Several works were conducted to decrease the loss induced by the cavity flow and increase the turbine performance by modifying the casing and shroud geometry. However, there is no specified geometrical parameter of a casing and shroud to increase the turbine performance. In this paper, a simple casing is suggested to increase turbine efficiency. The effect of casing geometry will be elucidated by analyzing the detailed cavity flow structure of each case.

## Chapter 2. Research method

### 2.1 Numerical model

In this study, turbine blade and shroud geometry are from the research project with Hanwha Aerospace. The stator has 35 blades and the rotor has 51 blades. Shroud has two labyrinth seals. Hub to tip ratio at the stator is 0.86 and that of at the rotor with the shroud is 0.84.

**Table 1 Turbine blade information**

	Stator	Rotor
Number of blades	35	51
Hub-to-tip ratio	0.86	0.84

Figure 7 shows the shroud geometry used in this work. The shroud has two labyrinth seals and it covers all the blade passage. The seal gap between the casing and the labyrinth seal is 1.3mm which is 2.2% of the span length.



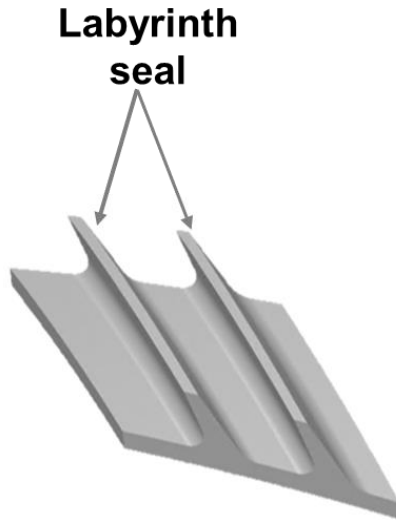


**Figure 7 Schematic of shroud geometry**

## **2.2 Numerical method**

The Ansys CFX 2020 R1 program is used to solve RANS equations. The mixing plane method is employed between the stator and rotor domain. Turbulence viscosity is calculated by the  $k - \omega$  shear stress transport (SST) model. The computational domain is filled up with tetrahedral mesh and added prism layer near the wall by the Ansys ICEM CFD.

The  $y^+$  value is in the range of 0.5 ~ 1.0 for the whole region. At the inlet, total temperature and total pressure are fixed. And the static pressure of outlet is given. A single passage computational domain with a single stator and rotor is used. The mesh elements are about 3 million in the stator and about 20 million in the rotor region.

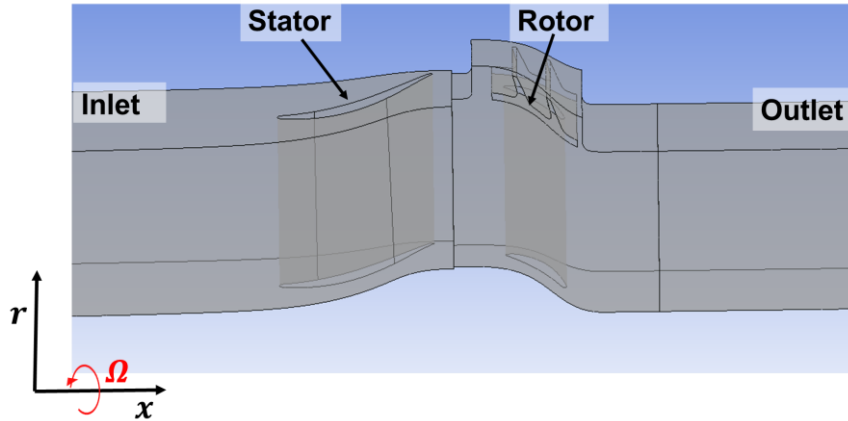


**Figure 8 Numerical computational domain: single passage**

## 2.3 Casing design

The casing designs are proposed to reduce the cavity mass flow rate and increase the turbine efficiency.

Figure 9 shows baseline geometry and Figure 10 indicate the two modified casing design, (a) slanted outlet cavity, and (b) stepped inlet cavity. The slanted outlet cavity case is proposed by adding slant inserts from the baseline case at the outlet cavity corner which reduces the outlet cavity volume. By reducing the outlet cavity volume, we intend to stagnate cavity flow and increase outlet cavity pressure. The stepped inlet cavity case is modified by adding a rectangular-shaped insert at the meridional view. This concept intends to block the leakage flow through the cavity and decrease its mass fraction.

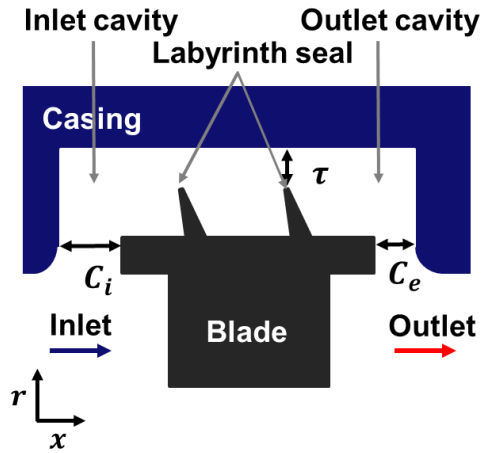


Figure 9 Schematic of the baseline case

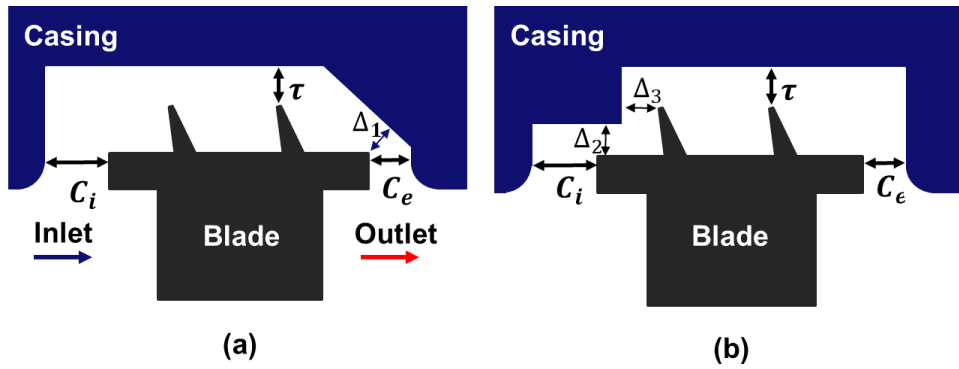


Figure 10 Schematic of modified casing design : (a) slanted outlet cavity (b) stepped inlet cavity

## Chapter 3. Results

CFD results are introduced and elucidated on how the aerodynamic performance changes occur in each case. There are significant changes in the turbine efficiency and cavity flow mass fraction. It is explained by analyzing the detailed flow structure of each case.

### 3.1 Cavity flow mass fraction and efficiency

The turbine efficiency is calculated by mass-averaged total pressure. The cavity mass flow is estimated by mass flow fraction in contrast to the main flow rate.

$$\text{Efficiency } \eta = \frac{\text{Power}}{\dot{m} C_p T_{t,in} \left(1 - \frac{P_{t,in}}{P_{t,out}}\right)^{\frac{\gamma-1}{\gamma}}} \quad (3.1)$$

$$\text{Cavity flow mass fraction} = \dot{m}_{leak} / \dot{m}_{main} \quad (3.2)$$

The efficiency of both modified cases is increased and the cavity flow mass fraction is decreased. In the slanted outlet cavity, the efficiency increases by 1.7%, and the cavity flow mass fraction decreases by 2.7%. In the stepped inlet cavity, the efficiency increase by 0.7% and the cavity flow mass fraction decrease by 2.7%. In both cases, the cavity flow mass fraction decreases at almost the same rate. However, the efficiency increases more in the slanted outlet case.

**Table 2 Numerically calculated efficiency and cavity flow mass fraction**

	Baseline	Slanted outlet cavity	Stepped inlet cavity
$\dot{m}_{leak}/\dot{m}_{main}(\%)$	8.4	5.7	5.7
$\eta(\%)$	85.4	87.1	86.4

### 3.2 Total pressure loss coefficient

$$Y_p = \frac{P_{t,in} - P_t}{P_{t,out} - P_{s,out}} \quad (3.3)$$

The loss through the turbine can be indicated by total pressure coefficient. Table 3 shows the loss coefficient 3 chord downstream from rotor. The total pressure loss coefficient is decreased in the slanted outlet cavity compared to the baseline. However, in the stepped inlet cavity, there is a negligible change of loss. The most of the efficiency change in the stepped inlet cavity is induced by an increase in torque not by the change of loss.

Figure 11 shows the loss coefficient of baseline case 0.5 chord downstream. There is a mixing zone that has most of the total pressure loss. Cavity flow at this region has lost its total pressure through the throttling process. Wake region is distributed through all spans.

Figure 12 and 13 shows the loss coefficient of modified casing design cases. In contrast to the baseline, there is negligible change under the tip region like the wake

and vortex region. However, in the mixing zone, Figure 13 presents an increased loss magnitude and a slightly larger loss region in the stepped inlet cavity case than the baseline. In a slanted outlet cavity, the loss magnitude and region are similar. In the stepped inlet cavity, the loss magnitude increases, and the loss region increases slightly.

**Table 3 Total pressure loss coefficient of each case(3.0 chord downstream from the rotor trailing edge)**

	Baseline	Slanted outlet cavity	Stepped inlet cavity
$Y_p$	8.4	5.7	5.7

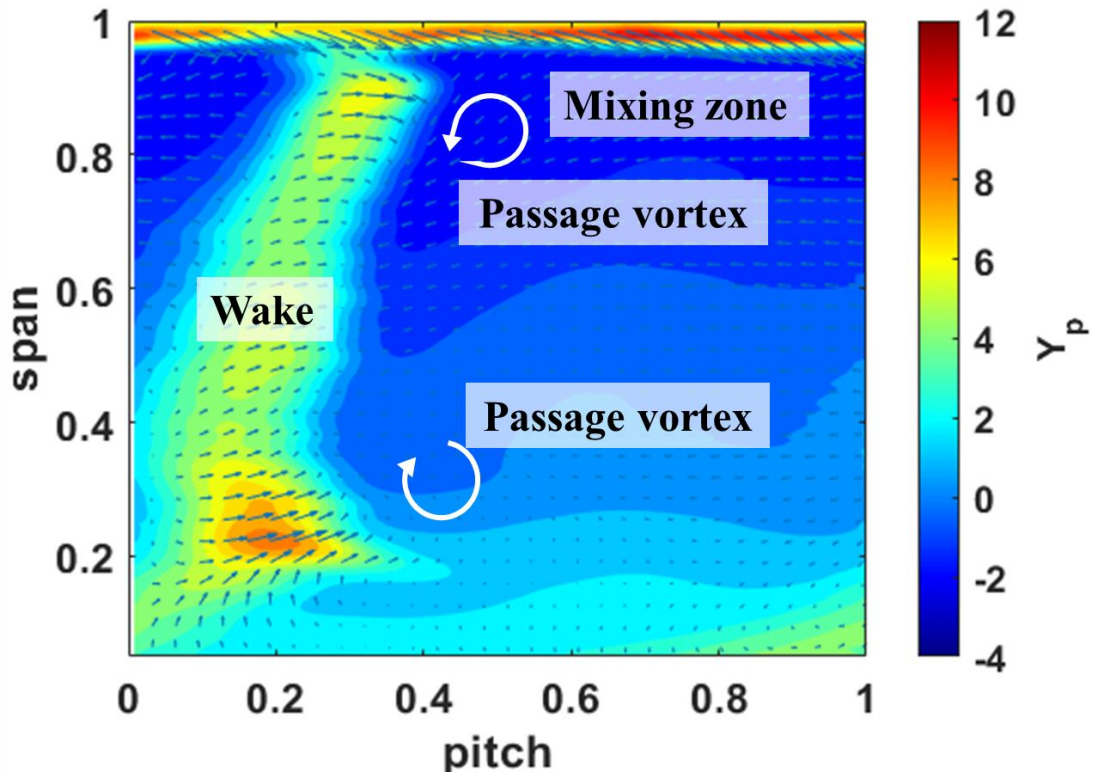


Figure 11 Total pressure loss coefficient of baseline  
(0.5 chord downstream from the rotor TE)

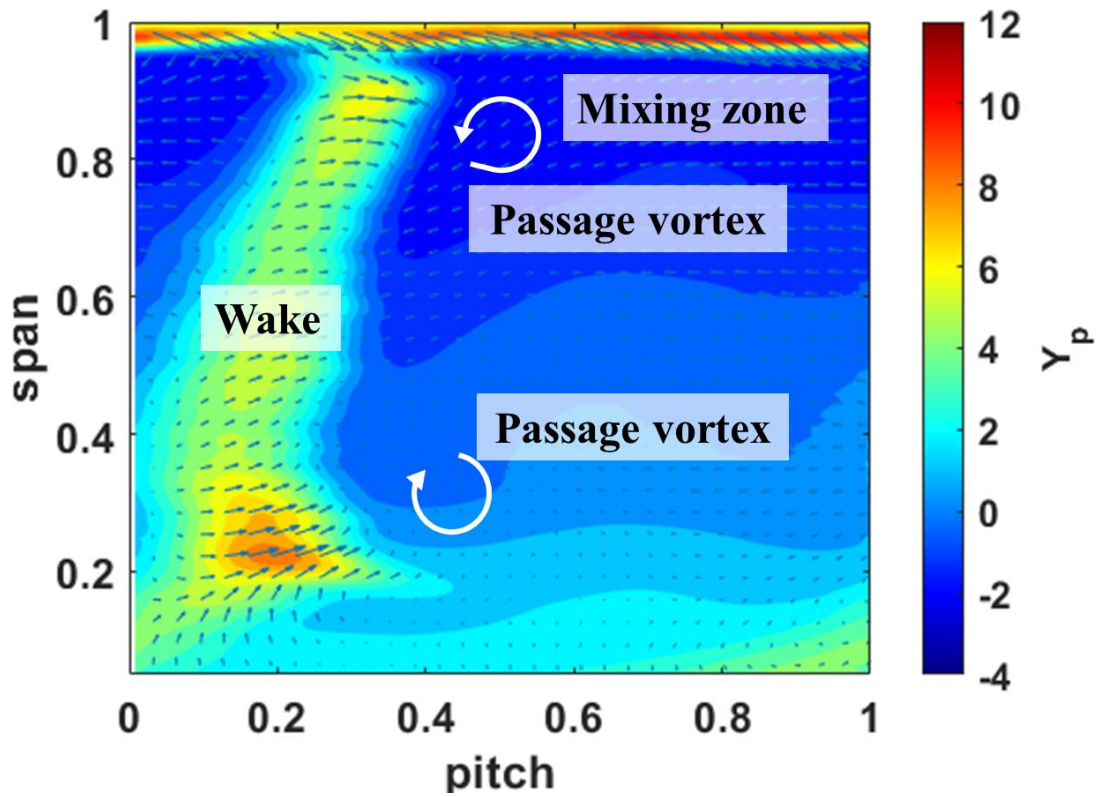


Figure 12 Total pressure loss coefficient of slanted outlet cavity  
(0.5 chord downstream from the rotor TE)



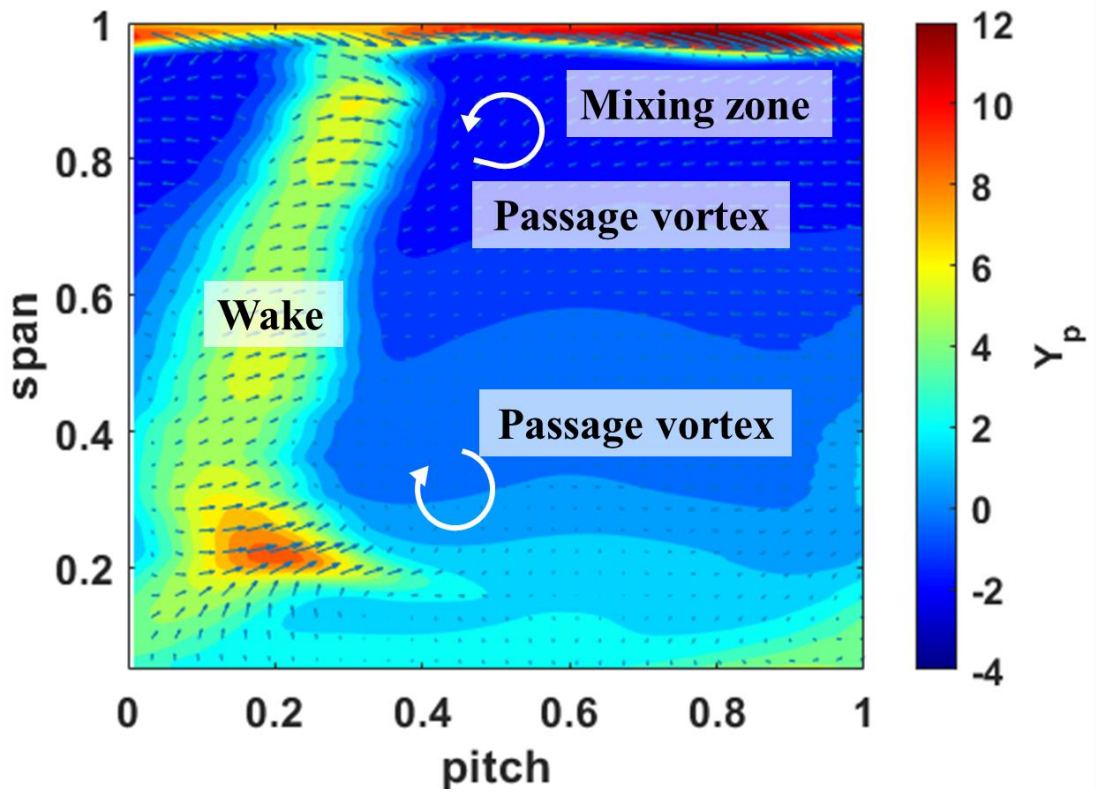


Figure 13 Total pressure loss coefficient of stepped inlet cavity  
(0.5 chord downstream from the rotor TE)

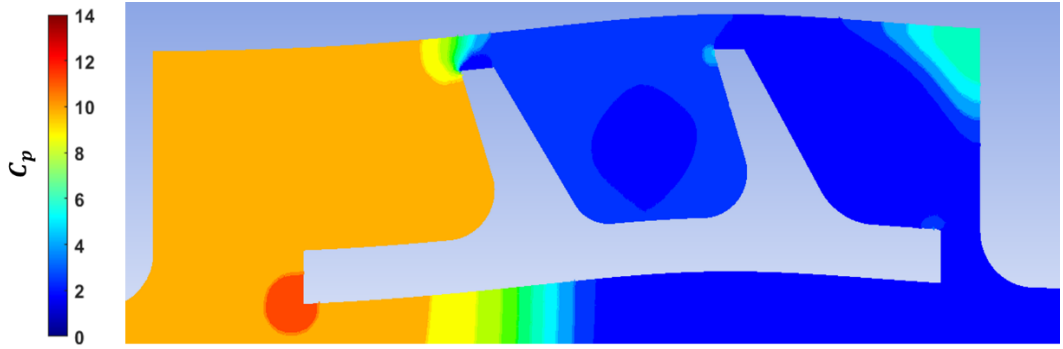
### 3.3 Pressure distribution

$$C_p = \frac{P_s - P_{s4}}{0.5\rho V_1^2} \quad (3.4)$$

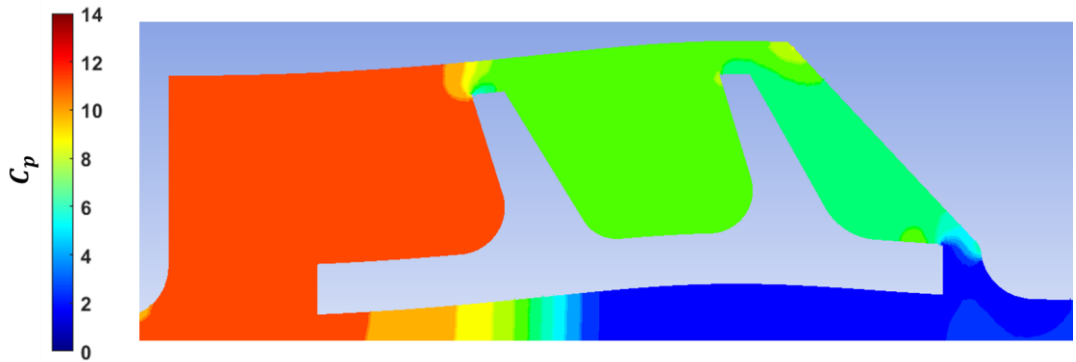
In a shrouded turbine, the pressure difference between the outlet cavity actuates cavity flow leaks through the cavity region. Hence the cavity flow mass fraction change in the slanted outlet cavity can be elucidated by the pressure distribution in cavity region.

Figure 15 shows the pressure distribution of the slanted outlet cavity case. The pressure at cavity exit is significantly increased compared to the baseline case pressure indicated in figure 14. Increased outlet cavity pressure is made from the separation at the cavity exit which induces pressure drop. Because pressure drop through rotor is fixed by main flow pressure drop rate, the pressure of cavity exit region increases. Increased cavity pressure reduces the cavity flow mass fraction.

In the stepped inlet cavity case, pressure drop rate through rotor cavity is similar with baseline. However, multi-separations induced by corners at the inlet cavity increase blockage. This effect reduces the cavity flow mass fraction.



**Figure 14 Cavity region pressure distribution of baseline**



**Figure 15 Cavity region pressure distribution of slanted outlet cavity**

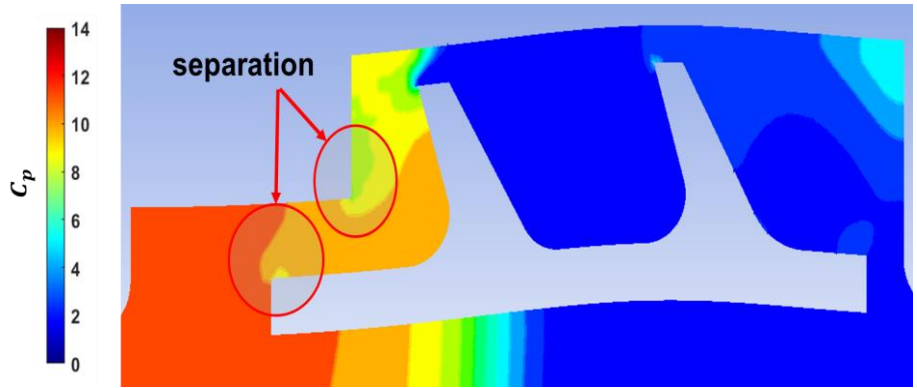


**Figure 16 Cavity region pressure distribution of stepped inlet cavity**

### 3.4 Torque

$$h_{t,2} - h_{t,1} = \Omega[(rc_{\theta})_1 - (rc_{\theta})_2] = \Omega r(c_{\theta,1} - c_{\theta,2}) \quad (3.5)$$

$$Torque = r(c_{\theta,1} - c_{\theta,2}) \quad (3.6)$$

Table 4 shows the torque worked on the rotor in modified cases obtained from the CFX Post program is significantly increased compared to the baseline case. The increased torque can be illustrated by the increased turning angle a difference between the relative inlet and outlet flow angle. Torque by flow angle indicates the torque calculated by the Euler turbine equation. These torque values are similar to the value of torque obtained from CFD Post and this shows that the most of efficiency increase is induced by increased torque in modified cases.

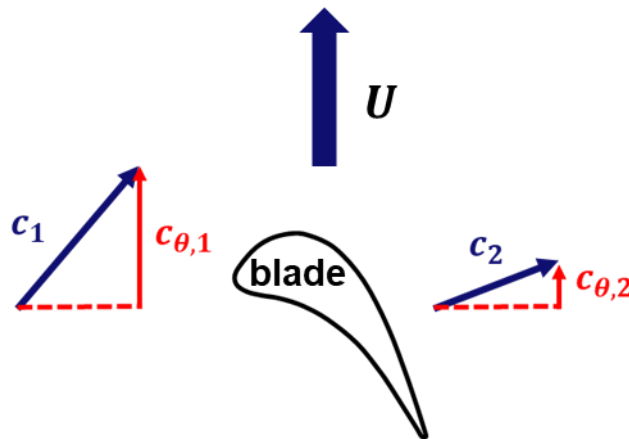


Figure 17 Flow schematics in the relative frame

**Table 4 Relative flow angle & torque calculated by flow angle**

	Baseline	Slanted outlet cavity	Stepped inlet cavity
Inlet flow angle	70.5	70.0	70.0
Outlet flow angle	22.1	17.2	17.1
Torque by flow angle (N · m)	8.395	8.902	8.924
Torque by CFD (N · m)	8.204	8.756	8.753

## Chapter 4. Conclusion

Two new casing designs are proposed to reduce cavity flow mass fraction and increase efficiency.

In the modified cases, cavity flow mass fraction are significantly reduced. For the slanted outlet cavity case, the modification of casing reduced the pressure drop through rotor cavity, Reduction of leakage flow is the beneficial effect of this reduced pressure drop. In the stepped inlet cavity, inlet cavity corners induce multiple separations. These separations work like blockage at the inlet cavity. The amount of decrease in cavity flow mass fraction is same in both cases. However, more loss generates by multiple separations in the stepped inlet cavity case at the cavity inlet.

Slanted edge in the outlet region and induced separation in the inlet cavity region work positively in reducing the cavity flow mass fraction. These simple design concepts make beneficial effects on shrouded turbine aerodynamic performance.

## Reference

- [1] Denton, J.D. "Loss Mechanisms in Turbomachines." Proceedings of the ASME 1993 International Gas Turbine and Aeroengine Congress and Exposition. Volume 2: Combustion and Fuels; Oil and Gas Applications; Cycle Innovations; Heat Transfer; Electric Power; Industrial and Cogeneration; Ceramics; Structures and Dynamics; Controls, Diagnostics, and Instrumentation; IGTI Scholar Award. Cincinnati, Ohio, USA. May 24–27, 1993. V002T14A001. ASME. <https://doi.org/10.1115/93-GT-435>
- [2] Porreca, L., Behr, T., Schlienger, J., Kalfas, A. I., Abhari, R. S., Ehrhard, J., and Janke, E. (March 1, 2004). "Fluid Dynamics and Performance of Partially and Fully Shrouded Axial Turbines." ASME. *J. Turbomach.* October 2005; 127(4): 668–678. <https://doi.org/10.1115/1.2008972>
- [3] Rosic, B., Denton, J. D., and Curtis, E. M. (June 17, 2008). "The Influence of Shroud and Cavity Geometry on Turbine Performance: An Experimental and Computational Study—Part I: Shroud Geometry." ASME. *J. Turbomach.* October 2008; 130(4): 041001. <https://doi.org/10.1115/1.2777201>
- [4] Rosic, B., Denton, J. D., Curtis, E. M., and Peterson, A. T. (June 17, 2008). "The Influence of Shroud and Cavity Geometry on Turbine Performance: An Experimental and Computational Study— Part II: Exit Cavity Geometry."



ASME. *J. Turbomach.* October 2008; 130(4):  
041002. <https://doi.org/10.1115/1.2777202>

- [5] Rosic, B., Denton, J. D., Curtis, E. M., and Peterson, A. T. (June 17, 2008). "The Influence of Shroud and Cavity Geometry on Turbine Performance: An Experimental and Computational Study— Part II: Exit Cavity Geometry." ASME. *J. Turbomach.* October 2008; 130(4): 041002. <https://doi.org/10.1115/1.2777202>
- [6] Schlienger, J, Pfau, A, Kalfas, AI, & Abhari, RS. "Effects of Labyrinth Seal Variation on Multistage Axial Turbine Flow." *Proceedings of the ASME Turbo Expo 2003, collocated with the 2003 International Joint Power Generation Conference. Volume 6: Turbo Expo 2003, Parts A and B.* Atlanta, Georgia, USA. June 16–19, 2003. pp. 173-185. ASME. <https://doi.org/10.1115/GT2003-38270>
- [7] Barmpalias, K. G., Abhari, R. S., Kalfas, A. I., Hirano, T., Shibukawa, N., and Sasaki, T. (May 31, 2012). "Design Considerations for Axial Steam Turbine Rotor Inlet Cavity Volume and Length Scale." ASME. *J. Turbomach.* September 2012; 134(5): 051031. <https://doi.org/10.1115/1.4004827>
- [8] Palmer, T. R., Tan, C. S., Zuniga, H., Little, D., Montgomery, M., and Malandra, A. (April 12, 2016). "Quantifying Loss Mechanisms in Turbine Tip Shroud Cavity Flows." ASME. *J. Turbomach.* September 2016; 138(9): 091006. <https://doi.org/10.1115/1.4032922>
- [9] Palmer, TR, Tan, CS, Zuniga, H, Little, D, Montgomery, M, & Malandra, A. "Quantifying Loss Mechanisms in Turbine Tip Shroud Cavity Flows." *Proceedings of the ASME Turbo Expo 2014: Turbine*

*Technical Conference and Exposition. Volume 2C: Turbomachinery.*  
Düsseldorf, Germany. June 16–20, 2014. V02CT38A021.  
ASME. <https://doi.org/10.1115/GT2014-25783>

- [10] Il Yun, Y., Porreca, L., Kalfas, A. I., Jin Song, S., and Abhari, R. S.  
(January 28, 2008). "Investigation of Three-Dimensional Unsteady  
Flows in a Two-Stage Shrouded Axial Turbine Using Stereoscopic  
PIV—Kinematics of Shroud Cavity Flow." ASME. *J. Turbomach.*  
January 2008; 130(1): 011021. <https://doi.org/10.1115/1.2720873>

## 초록

본 연구의 목적은 케이싱 형상이 쉬라우드형 터빈 성능에 어떤 영향을 미치는지를 조사하는 것이다. 케이싱 형상이 미치는 영향을 파악하기 위해 케이싱 형상의 변경을 한 케이스와 기존 형상 케이스에 대해 비교를 진행하였다. 케이싱 형상 변경을 통해 쉬라우드와 케이싱 사이의 공간에 해당하는 캐비티 공간의 변화를 주었다. 첫번째 형상은 인서트를 삽입하여 출구 캐비티 공간을 경사지게 만든 케이스이고 두번째 형상은 인서트를 삽입하여 계단 형태의 입구 캐비티 형상을 만든 케이스이다. 첫 번째 경우에는 스테이지 효율이 기준 형상에 비해 1.6% 증가하고 캐비티로 누설되는 질량 유량이 2.7% 감소하였다. 계단 형태의 입구 캐비티를 만든 두번째의 경우, 효율은 0.7% 증가하고 캐비티 유량은 2.7% 감소하였다. 두 경우 모두 누출 질량 유량을 줄임으로써 효율이 향상 되었다. 두 경우 모두 캐비티 누설 질량 유량을 줄임으로써 효율이 향상하였고 해당 논문에서는 상세한 유동구조 분석을 통해 캐비티 누설 유량이 감소한 원인과 효율 향상의 원인에 대해 설명하였다.

**핵심어:** 쉬라우드형 터빈, 케이싱 형상, 공력성능, 캐비티 누설유량

**학번:** 2021-23581